

# Reducing Energy Cost of NO<sub>x</sub> Production in Air Plasmas

X. Pei, D. Gidon and D. B. Graves

*Department of Chemical and Biomolecular Engineering, University of California - Berkeley, CA, USA*

**Abstract:** Air plasmas have been proposed for nitrogen fixation through production of NO<sub>x</sub> from air which can be readily converted to nitric acid. However, a major challenge remains in reducing the energy cost of NO<sub>x</sub> production in air plasmas to make the technology economically competitive. Different types of discharges such as arcs, sparks, dielectric barrier discharges have been investigated for NO<sub>x</sub> production, but they are challenging to compare due to differences in their structure, geometry and excitation modes etc. As of yet, there is no general evaluation criteria to determine the qualities of an appropriate discharge configuration for energy-efficient NO<sub>x</sub> production. In this study, we report on four types of discharges; dielectric barrier, glow, spark and extending arc discharge to examine NO<sub>x</sub> production efficiency under different conditions. Based on our results and previously published results from the literature, we elucidate a design rule to aid the construction of appropriate plasma sources for reduced energy cost NO<sub>x</sub> production.

**Keywords:** Nitrogen fixation, Atmospheric Pressure Air Plasma, NO<sub>x</sub> Production, Energy Cost.

## 1. Introduction

Reactive (or fixed) nitrogen (N<sub>r</sub>) is an essential component in synthetic fertilizers and is currently almost exclusively supplied via a chemical synthesis process (Haber-Bosch, or HB) originally developed in Germany in the first decade of the 20<sup>th</sup> century [1]. Nitrogen fertilizer generated via HB increased agricultural productivity to sustain nearly half of world population by the late 20<sup>th</sup> century. It accounts for about 1% of total world energy use and about 3-5% of worldwide conversion of natural gas is used to make the H<sub>2</sub> needed for the process. Since its inception in 1913, the HB process has been improved and refined. Modern, highly heat integrated HB plants use less than 30 GJ/tN (gigajoules expended per metric ton nitrogen produced) [2]. This value is remarkably close to the minimum thermodynamic limit of 24 GJ/tN. In spite of the obvious advantages of HB fertilizer manufacture, there are several significant problems with utilizing HB-manufactured synthetic fertilizer to meet current and future worldwide demand for N<sub>r</sub> including environmental issues, energy issues etc [3].

Before the HB process was invented in 1913, there were several commercial processes throughout the world that used air plasma to manufacture nitrogen based fertilizers. The best known process was the one developed and commercialized in the early 1900s by the Norwegian team of Birkeland and Eide [4]. Application of air plasma to directly create synthetic fixed nitrogen fertilizers - the Birkeland-Eide approach or some variation - would almost certainly not be economically effective today. Even with extensive advances in plasma technology it is unlikely that the air plasma process could be made economically competitive with HB. However, there are ways air plasma technology can complement HB without directly competing with it.

This concept has been described previously [5], but briefly, the proposed technology utilizes electrically-powered air plasma to create nitric oxide (NO). NO is readily oxidized under atmospheric air conditions to form NO<sub>2</sub>. When NO<sub>2</sub> is dissolved in water, primarily HNO<sub>3</sub> (in aqueous phase, nitrate anion NO<sub>3</sub><sup>-</sup>) is created. We envision using this aqueous NO<sub>3</sub><sup>-</sup> to treat nitrogen-containing organic waste such as manure or urine, lowering the pH to convert otherwise volatile NH<sub>3</sub> to involatile ammonium nitrate (i.e. NH<sub>4</sub>NO<sub>3</sub>). Volatile NH<sub>3</sub> is naturally created when bacteria break down organic forms of nitrogen in protein nucleic and amino acids. Use of nitric acid doubles the N-content of the organic fertilizer since for each molecule of NH<sub>3</sub> retained as NH<sub>4</sub><sup>+</sup>, a molecule of NO<sub>3</sub><sup>-</sup> is added. A key requirement for the competitiveness of this technology is the utilization of distributed plants of relatively small scale, located where organic waste is created and powered by locally produced renewable energy source.

It is clear that in order for the proposed technology to be commercially viable, the energy efficiency of the plasma process needs to be improved. The mechanisms of NO<sub>x</sub> formation in air plasma have been studied for many years in the context of atmospheric lightning discharge. More recently, several non-thermal plasma sources have been considered for nitrogen fixation [6-7]. These non-thermal sources are attractive as they typically have lower power requirements and are easier to operate. Various non-thermal plasma sources have been invested for NO<sub>x</sub> production with reported energy costs no lower than about 100-200 GJ/tN. It should be noted that a direct comparison of only energy cost per mass N<sub>r</sub> created is not necessarily the proper metric to judge the potential attractiveness of the proposed technology. The technology must be economically competitive of course, but it must also satisfy

many other constraints such as impact on the environment, appropriateness for a given local area and other factors.

In this study, we investigate four different types of discharges (DBD, glow, spark and arc type) in order to identify key parameters affecting the energy cost for NO<sub>x</sub> production and to guide design rules for discharge structures with improved performance. We first present the experimental set-ups and measurement methods we utilized in the study, followed by results regarding energy cost of NO<sub>x</sub> production under different discharge conditions. Finally we present a dimensionless parameter that appears to correlate energy cost of NO<sub>x</sub> production with a range of different discharges.

## 2. Experimental setups and measurements

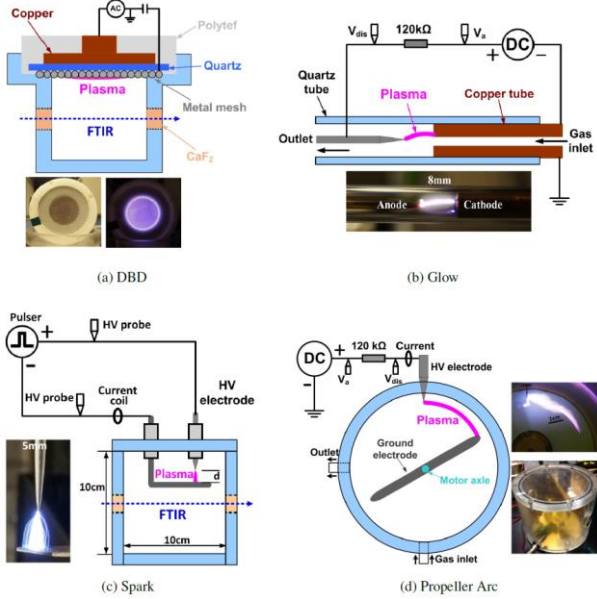


Fig. 1. Configurations and photos of experiment set up for NO<sub>x</sub> production using (a) DBD, (b) glow discharge, (c) spark discharge and (d) PA discharge.

Fig. 1(a) shows the schematic of DBD which consists of a cylindrical copper block (47 mm in diameter), used as the powered electrode, covered by a thin quartz plate (1 mm in thickness), which functions as a dielectric barrier. A wire mesh with a diameter of 0.5 mm and a mesh density of 88 meshes per cm<sup>2</sup> is situated on the quartz plate and used as ground electrode. More details can be found in [8]. The DC glow discharge has simple pin-to-plane configuration. Fig. 1(b) shows the configuration of the experimental set up for the DC glow discharge as well as a photo of a typical discharge condition with the gap distance set to 8 mm. The electrodes are situated in a quartz tube (ID 5 mm, OD 7 mm). A copper tube (ID 3 mm, OD 5 mm) is used as the cathode which doubles as the vent and fits flush inside the quartz tube. A tungsten needle, connected to the positive pole of a HV DC power supply (Spellman High Voltage, SL10PN1200) through a ballast resistor (120 kΩ), is used as the anode. The configuration of spark discharge is similar with glow discharge. A tungsten pin with a diameter of 1.6 mm is used as the anode and a copper plate

(10 mm x 100 mm) serves as the cathode as shown in Fig. 1(c). A nanosecond pulsed power supply (NSP-100, EHT) with a floating output stage is used as power supply which is capable of generating voltage amplitudes of up to 20 kV with a repetition rate up to 10 kHz, and a variable pulse width from 40 ns to 260 ns. Fig. 1(d) shows the configuration of extending-arc type source we termed Propeller Arc (PA), reported in our previous paper [9]. Briefly, PA consists of a rotating cathode (ground electrode), driven by a motor, with a fixed anode (HV electrode). Two propeller-like blades of cathode are made by stainless-steel. The distance between the center of motor axis and the tip of cathode is 35 mm. A stainless-steel pin with a diameter of 0.8 mm is used as the anode electrode.

Fourier Transform Infrared (FTIR) spectroscopy is performed as an in-situ diagnostic for NO<sub>x</sub> concentration in the different discharge configurations. The discharge powers are calculated based on the time integration of the discharge voltage and discharge current over one cycle. Then the energy cost of NO<sub>x</sub> production can be calculated.

In order to further understand the NO<sub>x</sub> production process, the average electric fields  $\bar{E}$  of the discharges are defined as:

$$\bar{E} = \frac{\int_{t_{bre}}^{\tau} \frac{V_{dis}(t)}{l} dt}{\tau - t_{bre}} \quad (1)$$

where  $V_{dis}(t)$  is the instantaneous gap discharge voltage and  $l$  the instantaneous visible length of the plasma.  $t_{bre}$  is the gap breakdown time.

Emission spectra from the N<sub>2</sub> second positive system is simulated and fitted to the measured optical emission spectra (OES) (via SpecAir software) to estimate rotational and vibrational temperatures of nitrogen.

## 3. Results

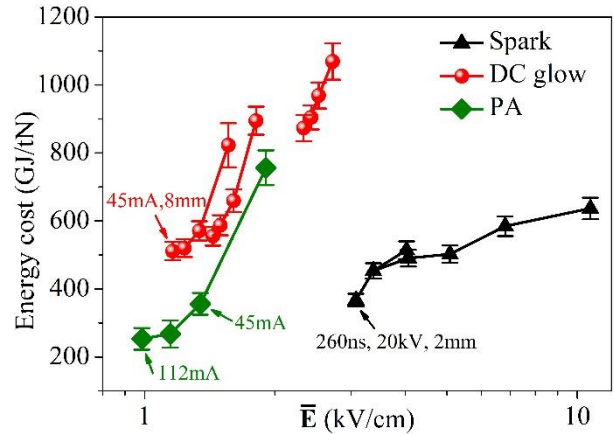


Fig. 2 Energy cost for NO<sub>x</sub> production in spark, glow and PA discharge with different conditions plotted as a function of  $\bar{E}$ .

We found that the DBD appears to not be suitable for NO<sub>x</sub> production from the view point of energy cost. The NO<sub>x</sub> production energy cost in the DBD (4000 GJ/tN to 10000 GJ/tN) is at least an order of magnitude larger than the other discharges investigated in this study. A

significant complication for the DBD nitrogen fixation is the abundant production of the greenhouse gas  $N_2O$ . We therefore focus our most discussion in the rest of the report to the three remaining discharges.

One clear result is that the energy cost, for each discharge type, tends to increase with increasing of  $\bar{E}$  as shown in Fig. 2. We note the results for the spark discharge (black triangles), do not follow the general correlation for the DC glow and PA, although the increasing trend between  $\bar{E}$  and energy cost is preserved.  $\bar{E}$  appears to be an important parameter to correlate the results we have collected, but it notably does not contain information about the thermal effects.

During our experiments, we found that the gas temperatures for each discharge are significantly different. To further analyze the  $NO_x$  production of different discharges, we bring the gas temperature into consideration and define the dimensionless parameter  $\chi$  (*Kai*) as follows:

$$\chi = \frac{\bar{E} \times \bar{T}}{E_r \times T_r} \quad (2)$$

where  $\bar{E}$  is calculated from (1) with units of kV/cm;  $\bar{T}$  is the average temperature estimated by OES with units of K;  $E_r$  and  $T_r$  are chosen to normalize the parameter at a reference condition. We choose (somewhat arbitrarily) the DC glow discharge with a gap distance of 5 mm and a discharge current of 45 mA as this reference condition. Since DC glow discharge has a simple and stable discharge character, the discharge conditions can be replicated easily for reference. The corresponding values of  $E_r$  and  $T_r$  1.43 kV/cm and 1800 K respectively.

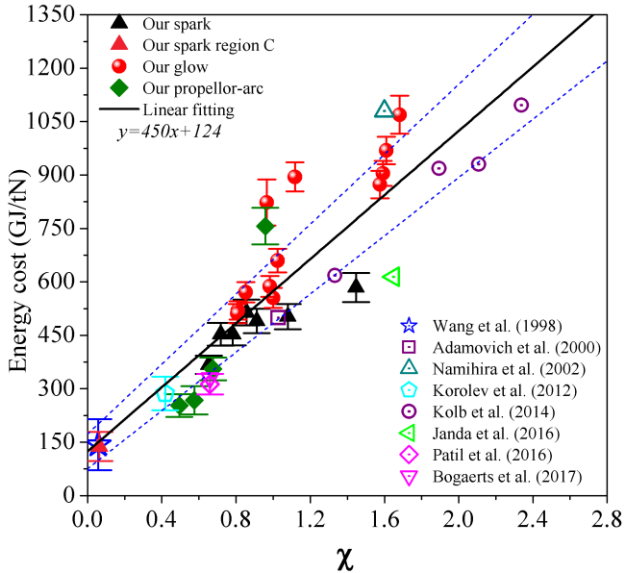


Fig. 3 Energy cost for  $NO_x$  production vary with  $\chi$  based on the reported works and our results using different plasma sources.

We also compute corresponding values of  $\chi$  and  $NO_x$  production costs from the literatures. We summarize the collected data as shown in Fig. 3. Note that all the data in Fig. 3 correspond to discharges at atmospheric pressure. Fig. 3 shows how the energy cost for  $NO_x$  production

varies with  $\chi$  for the different types of discharges. Remarkably, there is an almost linear relationship between  $\chi$  and energy cost for  $NO_x$  production. We conclude that reducing the value  $\chi$ , while maintaining a discharge, can be a guiding principle for reducing the energy cost of  $NO_x$  production.

We notice that the  $\chi$  factor seems related to the parameter reduced electric field  $E/N$  ( $E$  is the electric field strength,  $N$  is the gas density). The gas density  $N$  during discharge is generally difficult to measure due to simultaneous variations in gas pressure and gas temperature. Another key consideration is the transient and spatially distributed characteristics of  $E/N$  in these discharges. In fact, period-averaged  $E/N$  values corresponding to the lowest values of  $\chi$  in Fig. 3 would be too small to excite the key reactions for  $NO_x$  production, including  $N_2$  dissociation. Surprisingly, the  $\chi$  factor, as defined in (2), correlates with the energy cost of  $NO_x$  production for strikingly different types of discharges. This suggests  $\chi$  captures some implicit time and space dependent phenomena that must govern  $NO_x$  production in air discharges. Also, the  $\chi$  factor is relatively conveniently measured.

We also note that decreasing the  $\chi$  factor is not necessarily straightforward.  $\bar{E}$  and  $\bar{T}$  are often correlated in any particular discharge, and they cannot generally be directly manipulated. The applied voltage and the discharge (gap) voltage are not the same. The discharge voltage is a consequence of the gap distance, power supply characteristics and external circuit properties. Similarly,  $T$  varies with the electrical and thermal properties of the discharge. Higher currents typically lead to an increase in  $\bar{T}$ . In our ns-pulsed spark discharge, region C has very low  $\chi$  factor ( $\sim 0.06$ ), due to the high discharge current (20 A) corresponding to a low  $\bar{E}$  and extremely short discharge pulse (260 ns) preventing  $\bar{T}$  from increasing. However, in practice this region is necessarily preceded by a breakdown region, with a considerably larger  $\chi$  factor leading to a higher energy cost overall.

There are some possible paths to reduce the  $\chi$  factor. First, actively cooling the electrode or discharge surface (for example cooling by liquid nitrogen) may prove useful for reducing the  $\chi$  factor. Second, extending the plasma length  $l$  during operation, can reduce the  $\chi$  factor, as we have shown in our PA discharge. Last, using a high current peak and short duration (nanoseconds-microseconds) pulsed power can help reduce energy cost. We have demonstrated this effect with ns-pulsed spark discharge.

#### 4. Conclusions

Increasing the energy efficiency of nitrogen fixation using air plasmas should significantly advance their use as a novel technology to reduce the deleterious environmental impacts of growing fertilizer demand on the global nitrogen cycle. In this work, we investigated the energy cost of  $NO_x$  production using four types of discharges: DBD, glow, spark and PA in air. Additional details can be found elsewhere. [10]

Based on the results we presented here, we found the two key parameters controlling NO<sub>x</sub> production efficiency to be the average electric field  $\bar{E}$  and average gas temperature  $\bar{T}$ . Using these parameters we define the dimensionless parameter  $\chi$ , the normalized product of  $\bar{E}$  and  $\bar{T}$ . This quantity appears to effectively correlate specific energy cost of NO<sub>x</sub> production for the discharges we studied as well as results from the literature. Based on our results we conclude that reducing  $\chi$  could be a guiding principle in designing sources for energy-efficient NO<sub>x</sub> production. We suggest several methods to reduce  $\chi$ . One key insight is the need to reduce the energy cost associated.

The  $\chi$  factor appears to serve as a simple, effective means of correlating NO<sub>x</sub> production energy efficiency across a broad range of discharges. This indicates that  $\chi$  captures some intrinsic, but still poorly understood, physical and/or chemical mechanisms governing NO<sub>x</sub> production. Future research should focus on revealing these intrinsic mechanisms to further improve the practical attractiveness of air plasma for nitrogen fixation.

## 5. References

- [1] Y. Tanabe and Y. Nishibayashi, *Coordination Chemistry Reviews*, **257**, no.17-18, pp. 2551–2564, 2013.
- [2] V. Smil, Cambridge, Massachusetts: MIT Press, 2008.
- [3] J. G. Chen et al., *Science*, **360**, no. 6391, 2018.
- [4] N. Cherkasov et al., *Chemical Engineering and Processing: Process Intensification*, **90**, pp. 24–33, 2015.
- [5] D. B. Graves et al, *Plasma Medicine*, **5**, no. 2-4, pp. 257–270, 2015.
- [6] B. Patil et al., *Applied Catalysis B: Environmental*, **194**, pp. 123–133, 2016
- [7] M. A. Malik, *Plasma Chemistry and Plasma Processing*, **36**, no. 3, pp. 737–766, 2016.
- [8] M. J. Pavlovich et al., *Journal of Physics D-Applied Physics*, **46**, no. 14, 2013.
- [9] X. Pei et al., *Plasma Sources Science & Technology*, **27**(12) 125007, doi: 10.1088/1361-6595/aaf7ef, 2018.
- [10] X. Pei et al., *Chemical Engineering Journal*, **362**, 217-228, 2019.

## 6. Acknowledgements

The authors gratefully acknowledge many useful discussions with Rune Ingels of N2Applied (Oslo Norway). This work was partially supported by the US Department of Energy OFES grant DE-SC0001934, the US National Science Foundation Grant 1606062.